Available online at www.sciencedirect.com
SCIENCE DIRECT
Optical Fiber Technology 11 (2005) 111–130
Optical Fiber Technology
www.elsevier.com/locate/yofte

Invited paper

Integral form expansion of fiber Raman amplifier problem

Namkyoo Park *, Pilhan Kim, Jaehyoung Park, Lark Kwon Choi

Optical Communication Systems Laboratory, Seoul National University, Rm. 301-1101, San 56-1, Shilim, Kwanak, Seoul 151-742, South Korea

Received 4 November 2004

Abstract

We propose a novel fiber Raman amplifier (FRA) modeling method based on the expansion of the complicated Raman ordinary differential equation (ODE) into a closed integral/matrix form. By taking the effective length as the interim solution and updating its value along the iteration axis, Raman gain and pump/signal evolution can be calculated with orders of magnitude increase in convergence speed at the equivalent accuracy when compared to the previous approaches based on the direct numerical method for the ODE. Application of this formalism to the problem of (i) gain prediction with a given parameters, (ii) gain spectrum engineering for the search of optimum pump power set under the given constraints, (iii) gain clamping problem for the channel reconfiguration, and (iv) derivation of analytic formula for the faster FRA dynamic control have been addressed.

Keywords: Optical amplifier; Raman; Algorithm; Gain control; Optimization methods; Integral equations

1. Introduction

The fiber Raman amplifier (FRA) has become an indispensable technology with its distinctive advantages—such as flexible gain bandwidth and intrinsically lower noise characteristics [1,2]. For the optimal design of the Raman amplifier/amplified transmission

* Corresponding author. Fax: +82-2-885-5284.
E-mail address: nkpark@plaza.snu.ac.kr (N. Park).

1068-5200/$ – see front matter
doi:10.1016/j.yofte.2005.01.001

systems, various approaches have been proposed for the efficient/accurate modeling of the Raman amplifier [3–6]. Although different in their algorithm details, levels of convergence speed and accuracies, still all these approaches share the common platform of coupled ordinary differential equations (ODE) for the Raman equation set that must be solved along the long length of fiber propagation axis, resulting exhaustive calculation efforts.

In this work, we introduce an alternative, highly efficient modeling method for FRA analysis. By formulating the coupled ODEs for general FRA problem to a closed recursive form based on the integral equation, Raman amplifier is solved along the iteration axis rather than the fiber axis, enabling orders of faster convergence speed at the equivalent accuracy achievable with the previous approaches. With this platform, we show that the traditional FRA problems such as (i) gain prediction with a given parameters, (ii) gain spectrum engineering for the search of optimum pump power set under the given constraints, and (iii) gain clamping under the channel reconfiguration can be treated in a much simpler/faster way.

2. Closed form expansion of Raman equation

To construct such an algorithm/platform stated in the introduction, we treat the Raman gain coefficient as the perturbation factor in the adiabatic process and (1) derive a recursive relation of Raman integral equation, (2) construct a matrix formalism for the efficient calculation of the relations.

2.1. Formulation

Focusing to the conventional, distributed FRA which use long length of transmission fiber as the gain medium, the effect of amplified spontaneous emission (ASE) and Rayleigh scattering can be ignored in good approximation [1,7]. Under these assumptions (which will be justified later), the coupled nonlinear Raman processes between waves in the fiber can be expressed as [7–9]

$$\pm\frac{dP_i}{dz} = -\alpha_i P_i + \sum_{j=1}^{M+N} g_{ji} P_j P_i,$$
$$g_{ji} = \begin{cases} \frac{g_R(\nu_j-\nu_i)}{2A_{\mathrm{eff}}} & \text{when } j \leqslant i, \\ -\left(\frac{\nu_i}{\nu_j}\right)\frac{g_R(\nu_i-\nu_j)}{2A_{\mathrm{eff}}} & \text{when } j > i, \end{cases} \tag{1}$$

where P_i is the power of ith wave, α_i is the attenuation coefficient, $g_R(\Delta\nu)$ is the Raman gain coefficient between waves separated by $\Delta\nu$, A_{eff} is the effective area, M is the number of pumps, and N is the number of signal waves. After dividing Eq. (1) by P_i and integrating over z, we get

$$P_i(z) = P_i(0)\exp\left[\mp\alpha_i z \pm \left(\sum_{j=1}^{M+N} g_{ji} \int_0^z P_j(\zeta)\,d\zeta\right)\right]. \tag{2}$$

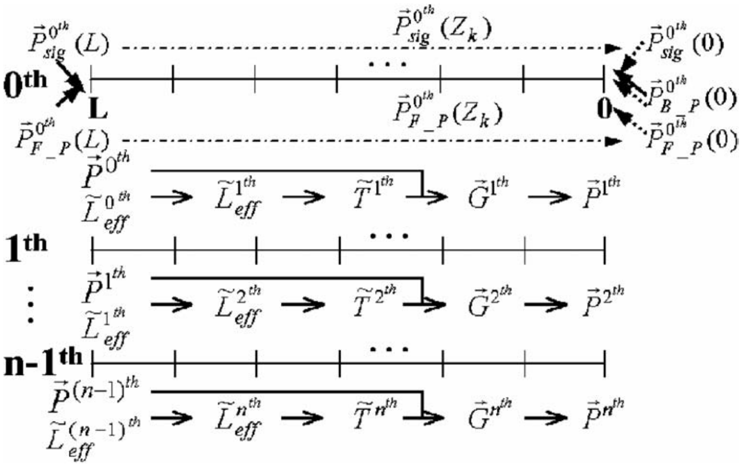

Fig. 1. Flow diagram of the suggested adiabatic iteration algorithm along the iteration axis. ($\vec{P}^{(0)}_{\mathrm{sig}}$, $\vec{P}^{(0)}_{\mathrm{F,P}}$, $\vec{P}^{(0)}_{\mathrm{B,P}}$; zeroth-order signal, forward-pump, and backward-pump power.)

Here, the upper/bottom signs are for the forward/backward propagating waves, respectively. With an additional integration process, we get the following integral form of Raman wave equations:

$$\frac{\int_0^z P_i(\zeta)\,d\zeta}{P_i(0)} = \int_0^z \exp\left[\mp\alpha_i\zeta \pm \left(\sum_{j=1}^{M+N} g_{ji}\int_0^{\zeta} P_j(\xi)\,d\xi\right)\right]d\zeta. \tag{3}$$

Now, utilizing the definition of $L_{\mathrm{eff},i}(z) = \int_0^z P_i(\zeta)/P_i(0)\,d\zeta$, we can then rewrite Eq. (3) into a closed integral form for the effective length,

$$L_{\mathrm{eff},i}(z) = \int_0^z \exp\left[\mp\alpha_i\zeta \pm \left(\sum_{j=1}^{M+N} g_{ji}P_j(0)L_{\mathrm{eff},j}(\zeta)\right)\right]d\zeta. \tag{4}$$

To solve this equation, we apply Picard's iteration method to Eq. (4) taking $L_{\mathrm{eff},i}$ as the interim target solution. At nth iteration step, Eq. (4) becomes

$$L^{(n)}_{\mathrm{eff},i}(z) = \int_0^z \exp\left[\mp\alpha_i\zeta \pm \left(\sum_{j=1}^{M+N} g_{ji}P^{(n-1)}_j(0)L^{(n-1)}_{\mathrm{eff},j}(\zeta)\right)\right]d\zeta. \tag{5}$$

For the implementation of the above equations into the numerical domain, we now construct a vector $\tilde{L}^{(n)}_{\mathrm{eff},i}(\vec{z}_k)$ to assign the value of the effective length at the ith wavelength at the position vector z_k (the discrete position element covering the whole fiber link with step size of Δz, as shown in Fig. 1), with the vector elements,

$$L^{(n)}_{\mathrm{eff},i}(\vec{z}_k) = \exp\left[\mp\alpha_i\vec{z}_k \pm \left(\vec{g}_{ji}\vec{P}^{(n-1)}_j(0)\right)\cdot\tilde{L}^{(n-1)}_{\mathrm{eff},j}(\vec{z}_k)\right]\cdot\tilde{T}_{\mathrm{trig}}\cdot\Delta z, \tag{6}$$

where

$$\vec{z}_k = [0 \quad \Delta z \quad 2\Delta z \quad 3\Delta z \quad \ldots \quad L-\Delta z \quad L],$$

$$L_{\mathrm{eff},i}^{(n)}(\vec{z}_k) = \left[\, L_{\mathrm{eff},i}^{(n)}(0) \quad L_{\mathrm{eff},i}^{(n)}(\Delta z) \quad L_{\mathrm{eff},i}^{(n)}(2\Delta z) \quad \ldots \quad L_{\mathrm{eff},i}^{(n)}(L)\,\right],$$

$$\vec{g}_{ji}\vec{P}_j^{(n-1)}(0) = \left[\, g_{1i}P_1^{(n-1)}(0) \quad g_{2i}P_2^{(n-1)}(0) \quad g_{3i}P_3^{(n-1)}(0) \quad \ldots \quad g_{(M+N)i}P_{M+N}^{(n-1)}(0)\,\right],$$

$$\tilde{L}_{\mathrm{eff},j}^{(n-1)}(\vec{z}_k) = \begin{bmatrix} L_{\mathrm{eff},1}^{(n-1)}(0) & L_{\mathrm{eff},1}^{(n-1)}(\Delta z) & L_{\mathrm{eff},1}^{(n-1)}(2\Delta z) & \cdots & L_{\mathrm{eff},1}^{(n-1)}(L) \\ L_{\mathrm{eff},2}^{(n-1)}(0) & L_{\mathrm{eff},2}^{(n-1)}(\Delta z) & L_{\mathrm{eff},2}^{(n-1)}(2\Delta z) & \cdots & L_{\mathrm{eff},2}^{(n-1)}(L) \\ L_{\mathrm{eff},3}^{(n-1)}(0) & L_{\mathrm{eff},3}^{(n-1)}(\Delta z) & L_{\mathrm{eff},3}^{(n-1)}(2\Delta z) & \cdots & L_{\mathrm{eff},3}^{(n-1)}(L) \\ \vdots & \vdots & \vdots & \vdots & \vdots \\ L_{\mathrm{eff},(M+N)}^{(n-1)}(0) & L_{\mathrm{eff},(M+N)}^{(n-1)}(\Delta z) & L_{\mathrm{eff},(M+N)}^{(n-1)}(2\Delta z) & \cdots & L_{\mathrm{eff},(M+N)}^{(n-1)}(L) \end{bmatrix},$$

$$\tilde{T}_{\mathrm{trig}} = \begin{bmatrix} 0 & 1/2 & 1/2 & 1/2 & \cdots & 1/2 \\ 0 & 1/2 & 1 & 1 & \cdots & 1 \\ 0 & 0 & 1/2 & 1 & \cdots & 1 \\ 0 & 0 & 0 & 1/2 & \cdots & 1 \\ \vdots & \vdots & \vdots & \vdots & \vdots & \vdots \\ 0 & 0 & 0 & 0 & \cdots & 1/2 \end{bmatrix}.$$

Meanwhile, utilizing the rule of superposition with fractional Raman gains [7–9], the Raman gain at a certain wavelength can be expressed as

$$G_i = \sum_{j=1}^{M+N} g_{ji} \cdot L_{\mathrm{eff},j}(L) \cdot P_j(0). \tag{7}$$

Treating the power $P_j(0)$ of signal/pump waves as an individual vector element, we now transform the gain Eq. (7) into following matrix form:

$$\vec{G} = \tilde{T} \times \vec{P}, \tag{8}$$

where

$$\vec{G} = \begin{bmatrix} G_1 \\ G_2 \\ \vdots \\ G_{N+N} \end{bmatrix},$$

$$\tilde{T} = \begin{bmatrix} g_{11}L_{\mathrm{eff},1}(L) & g_{21}L_{\mathrm{eff},2}(L) & \cdots & g_{(M+N)1}L_{\mathrm{eff},(M+N)}(L) \\ g_{12}L_{\mathrm{eff},1}(L) & g_{22}L_{\mathrm{eff},2}(L) & \cdots & g_{(M+N)2}L_{\mathrm{eff},(M+N)}(L) \\ \vdots & \vdots & \vdots & \vdots \\ g_{1(M+N)}L_{\mathrm{eff},1}(L) & g_{2(M+N)}L_{\mathrm{eff},2}(L) & \cdots & g_{(M+N)(M+N)}L_{\mathrm{eff},(M+N)}(L) \end{bmatrix},$$

$$\vec{P} = \begin{bmatrix} P_1(0) \\ P_2(0) \\ \vdots \\ P_{N+N}(0) \end{bmatrix}.$$

Utilizing these formulations, the Raman gain values for every pump/signal waves can be obtained with a matrix multiplication process without relying on a complex solution search procedure of the coupled ODEs.

2.2. *Application example 1: Gain prediction*

The actual procedure to practically implement the above-derived analytic formulation into the numerical domain can be summarized as follows.

Step 1. Initial condition setup

Treating the $g_{ji} \times P_j(0) \times L_{\mathrm{eff},j}(\vec{z}_k)$ in Eq. (6) as a perturbation parameter in the adiabatic process, we first assume it to be zero for the zeroth iteration step to get the zeroth-order initial effective length, $\tilde{L}^{(0)}_{\mathrm{eff},j}(\vec{z}_k) = (1 - \exp(\mp\alpha_j \vec{z}_k))/\alpha_j$. At the same time, to ease the application of transfer matrix for all forward/backward propagating waves, we treat the forward propagating waves injected at the input end ($z = L$) as the backward propagating waves assigned to the output end [5] ($z = 0$, as illustrated in Fig. 1). Under this arrangement, for the forward propagating waves in the counter-/bi-directional pumping configuration, we can set the initial guess of the signal power at the output end ($\vec{P}^{(0)}_{\mathrm{sig}}(0)$) and forward pump power at the output end ($\vec{P}^{(0)}_{\mathrm{F,P}}(0)$) to be equal to ($\vec{P}^{(0)}_{\mathrm{sig}}(L) - |\text{fiber loss}|$) and ($\vec{P}^{(0)}_{\mathrm{F,P}}(L) - |\text{fiber loss}|$), respectively. Here, the signal power at the input end $\vec{P}^{(0)}_{\mathrm{sig}}(L)$ and forward pump power at the input end $\vec{P}^{(0)}_{\mathrm{F,P}}(L)$ are simply the pre-determined initial value (already known). As can be easily figured out, in the co-directional pumping configuration, we can use the pre-determined initial input signal power and forward pump power as $\vec{P}^{(0)}_{\mathrm{sig}}(0)$ and $\vec{P}^{(0)}_{\mathrm{F,P}}(0)$, respectively, by simply assigning the z values from the opposite direction.

Step 2. Calculation of higher-order terms

By substituting $\vec{P}^{(0)}(0)$ and $\tilde{L}^{(0)}_{\mathrm{eff},j}(L)$ into Eq. (6), the first-order approximation for the effective length $\tilde{L}^{(1)}_{\mathrm{eff},j}(L)$ can be obtained. Also can be obtained is the value of $\vec{G}^{(1)}$ from $\vec{P}^{(0)}(0)$ and $\tilde{T}^{(1)}$ (calculated from $\tilde{L}^{(1)}_{\mathrm{eff},j}(L)$) by Eq. (8). Finally, to get the first-order value of the target solution $\vec{P}^{(1)}(0)$ in the counter-/bi-directional pumping configuration, we set $\vec{P}^{(1)}_{\mathrm{sig}}(0)$ and $\vec{P}^{(1)}_{\mathrm{F,P}}(0)$ equal to ($\vec{P}^{(0)}_{\mathrm{sig}}(L) - |\text{fiber loss}| + \vec{G}^{(1)}$) and ($\vec{P}^{(0)}_{\mathrm{F,P}}(L) - |\text{fiber loss}| + \vec{G}^{(1)}$), respectively.

Step 3. Reiteration

Repeating the iteration procedure described in Step 2 at the higher-order values of $\tilde{L}^{(n)}_{\mathrm{eff},j}(L)$, $\tilde{T}^{(n)}$, $\vec{G}^{(n)}$, $\vec{P}^{(n)}(0)$, and $\vec{P}^{(n)}(L)$, as shown in Fig. 1, the converged final solution set can be obtained.

Figures 2 and 3 show the comparison result between the described algorithm and the conventional average power method [5]. 71 signals were used at the wavelength of 1530–1600 nm with 1 nm spacing at the signal power of -13 dB m/ch. For the co-/counter-directional pumping scheme, we used 14 pumps (1420–1480 nm with 5 nm spacing, and an additional pump at 1495 nm), while for the bi-directional scheme we tested with 4 pumps in the forward direction (1420–1435 nm with 5 nm spacing) and 10 pumps in the backward direction (1440–1480 nm with 5 nm spacing and 1495 nm). 37 km of dispersion shifted fiber (DSF), which has a larger Raman gain coefficient than that of single mode fiber (SMF), was employed as the test gain medium. As can be seen from Fig. 2, the suggested method shows excellent convergence accuracy—after 6 iteration steps, and the accuracy improvement from the next order of iteration becomes less than 0.002 dB. The relative gain difference between the proposed method and the average power method (APA) including the effects from the ASE and Rayleigh scattering (scattering loss $6 \times 10^{-5}\ \mathrm{m}^{-1}$, recapture fraction 10^{-3}) remained less than 0.03 dB over the whole 71 nm gain spectral range at the similar level of convergence (gain accuracy improvement <0.002 dB).

Meanwhile, the required computation time to get the exact Raman gain and signal/pump power distribution was less than 1 s (at 100 m of spatial resolution) for all the co-, counter-, and bi-directionally pumping configurations, with a conventional PC (2.0 GHz CPU clock). To note, the measured convergence speed of the APA method (without ASE and Rayleigh scattering, for the fair comparison) was much longer (order of 10^2 s, at much lower spatial resolution of 1.85 km, number of iteration $= 4$, used fourth-order Runge–Kutta method at 300 K). Figure 3 also shows the signal evolution along the fiber. The excellent agreements between the two simulation results show the validity of the proposed algorithm.

Now, from the acquired signal/pump distribution, various FRA noise also can be obtained by expanding the well-known formula [10] to include multi-wavelength pump as follows:

$$\begin{aligned}
P_{\mathrm{ASE}^+}(\nu_\mathrm{s}, z) = \sum_{\text{pumps}} & G_{\mathrm{net}}(\nu_\mathrm{s}, z) \\
& \times \int_{\zeta=0}^{z} (1+\eta_\mathrm{T}) 2h\nu_\mathrm{s} B_\mathrm{o} g_\mathrm{R}(\nu_\mathrm{p}-\nu_\mathrm{s}) P_\mathrm{p}(\nu_\mathrm{p}, \zeta) \frac{1}{G_{\mathrm{net}}(\nu_\mathrm{s}, \zeta)}\, d\zeta,
\end{aligned}$$

$$P_{\mathrm{ASE}^-}(\nu_\mathrm{s}, z) = \sum_{\text{pumps}} \frac{1}{G_{\mathrm{net}}(\nu_\mathrm{s}, z)} \int_{\zeta=z}^{L} (1+\eta_\mathrm{T}) 2h\nu_\mathrm{s} B_\mathrm{o} g_\mathrm{R}(\nu_\mathrm{p}-\nu_\mathrm{s}) P_\mathrm{p}(\zeta) G_{\mathrm{net}}(\nu_\mathrm{s}, \zeta)\, d\zeta,$$

$$P_{\mathrm{ASE}^-}^{\mathrm{R}}(\nu_\mathrm{s}, z) = G_{\mathrm{net}}(\nu_\mathrm{s}, z) \int_{\zeta=0}^{z} \left(S\alpha_\mathrm{s}^{\mathrm{R}}\right) P_{\mathrm{ASE}^-}(\nu_\mathrm{s}, \zeta) \frac{1}{G_{\mathrm{net}}(\nu_\mathrm{s}, \zeta)}\, d\zeta,$$

$$\begin{aligned}
P_\mathrm{s}^{\mathrm{DRS}}(\nu_\mathrm{s}, z) = G_{\mathrm{net}}(\nu_\mathrm{s}, z) \left(S\alpha_\mathrm{s}^{\mathrm{R}}\right)^2 P_\mathrm{s}(\nu_\mathrm{s}, 0) & \int_{\zeta=0}^{z} \frac{1}{(G_{\mathrm{net}}(\nu_\mathrm{s}, \zeta))^2} \\
& \times \int_{\xi=\zeta}^{L} \left(G_{\mathrm{net}}(\nu_\mathrm{s}, \xi)\right)^2 d\xi\, d\zeta,
\end{aligned}$$

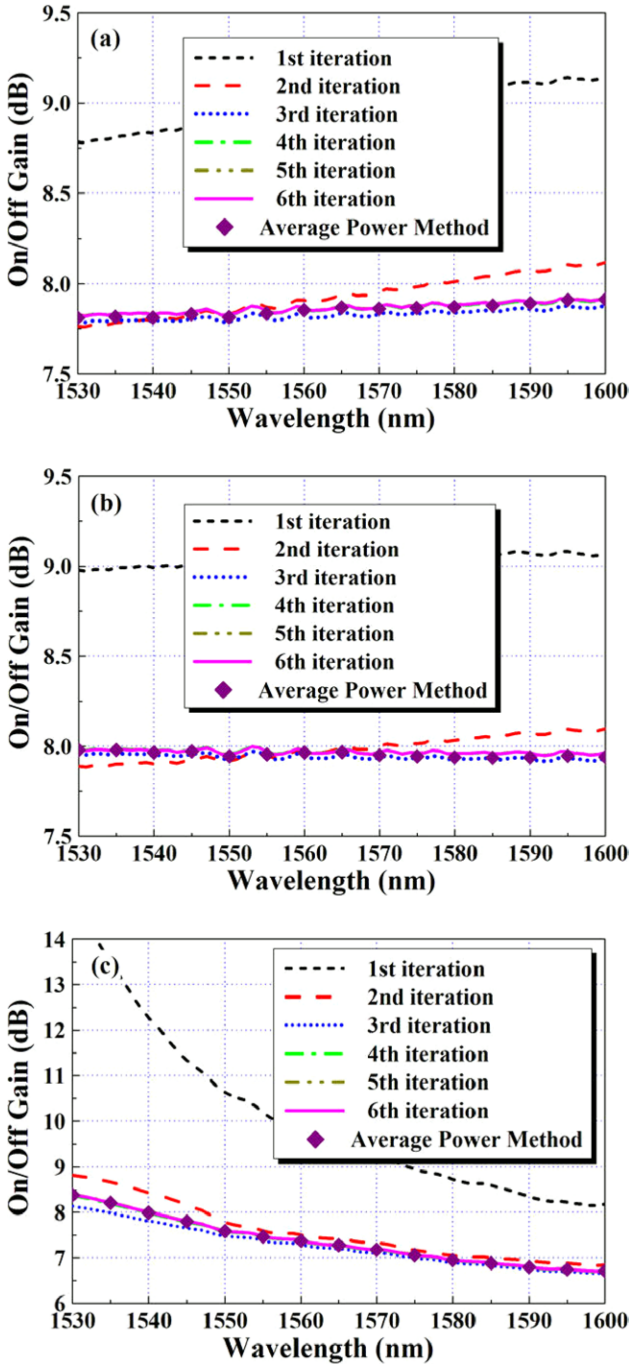

Fig. 2. Raman on/off gain with different pumping configurations: (a) co-directional, (b) counter-directional, and (c) bi-directional pumping.

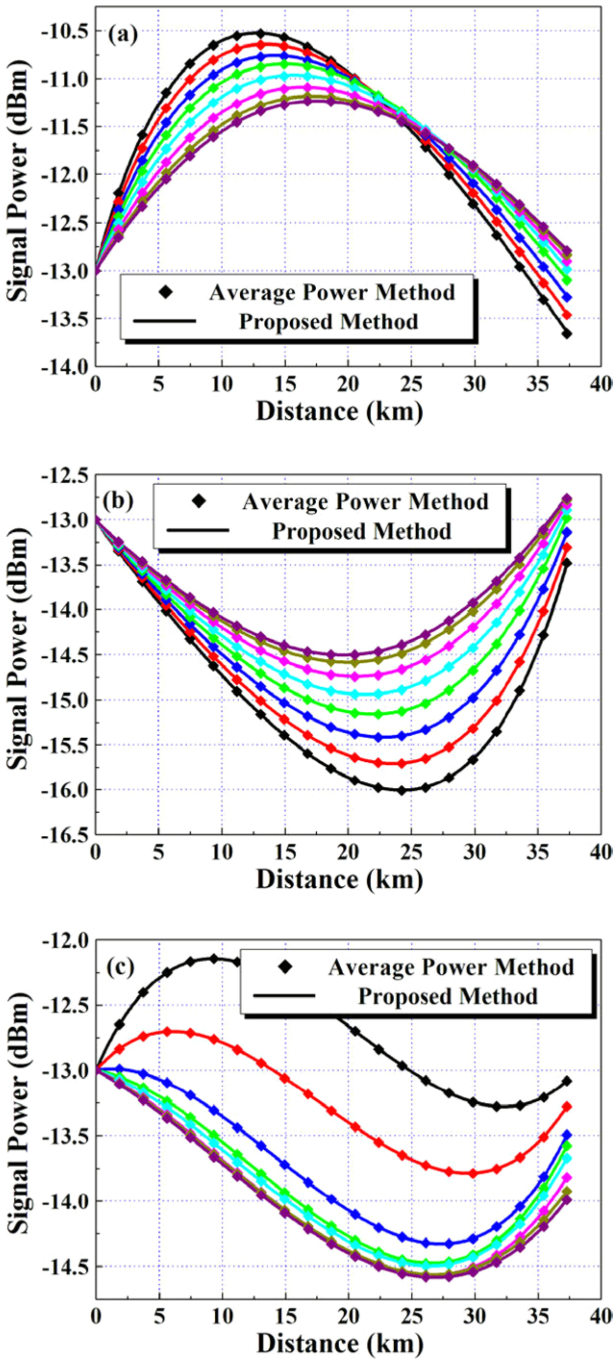

Fig. 3. Signal power evolution at 1530–1600 nm with 10 nm spacing: (a) co-directional, (b) counter-directional, and (c) bi-directional pumping.

where $G_{\mathrm{net}}(\nu_s, z)$ and $P_s(\nu_s, z)$ are the distribution of net-gain and signal power, respectively, $P_p(\nu_p, z)$ is the distribution of pump power, η_T is the thermal equilibrium excitation equal to $1/(\exp(h(\nu_p - \nu_s)/kT) - 1)$, B_o is the optical bandwidth, α_s^R is the Rayleigh scattering loss, and S is the recapture fraction. Figure 4 shows the examples of noise calculation (scattering loss $6 \times 10^{-5}\ \mathrm{m}^{-1}$, recapture fraction 10^{-3} at 300 K, resolution bandwidth $= 0.5$ nm).

It is worth to note that, above result can be as well used to estimate the accumulated ASE power for cascaded FRA links. Applying the well-known formula (multiplying the number of cascade to the ASE power of single stage), the output ASE power after 10 spans of FRA link can be obtained (Fig. 5a). As can be seen, the result agrees remarkably well with the accumulated ASE power obtained with the full APA method. Figure 5b shows the comparison of gain spectrum between the standard model (including both ASE and Rayleigh

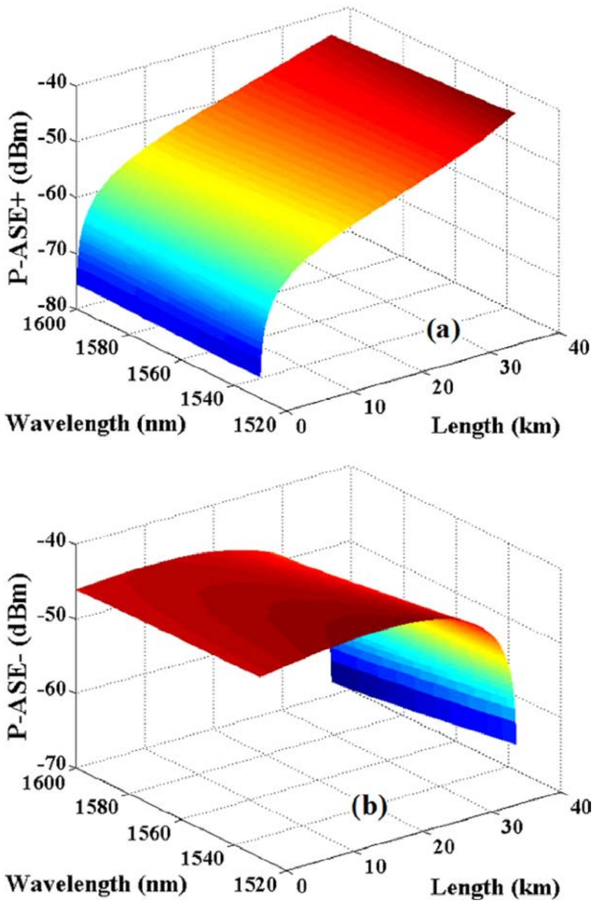

Fig. 4. Various FRA noise component in the counter-pumping configuration: (a) forward ASE power, (b) backward ASE power, (c) Rayleigh-scattered backward ASE power, and (d) double Rayleigh back-scattered signal power.

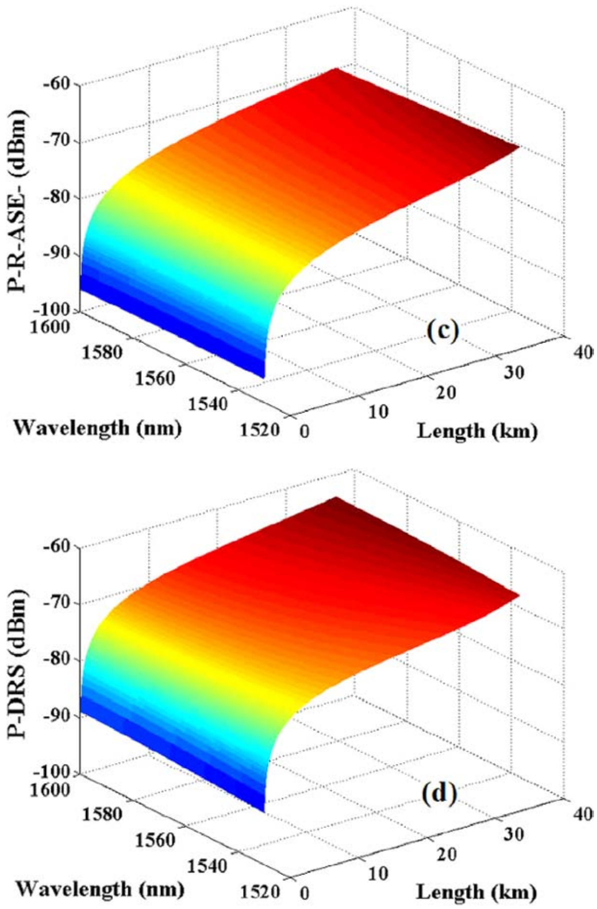

Fig. 4. (Continued.)

scattering—showing the gain decreases from the ASE accumulation/gain depletion effect from cascade) and our method (including the ASE depletion obtained from Fig. 5a), after first and tenth FRA cascade. The relative gain error between those two methods remained still within 0.03 dB after 10 span of FRA.

2.3. Application example 2: Raman gain engineering—The inverse problem

Out of many distinctive advantages that the Raman fiber amplifier (RFA) provides, the flexibility in gain engineering can be considered to be one of the key advantages that other types of amplifiers cannot provide. Still, there exists an additional difficulty in the gain profile design of FRA, when compared to other types of optical amplifiers: the strong interactions of pump waves inside the FRA make it difficult to predict the required pump power sets for the target gain profile [4]. To back trace the pump powers required for the target design, one has to iteratively adjust the pump input powers by using either

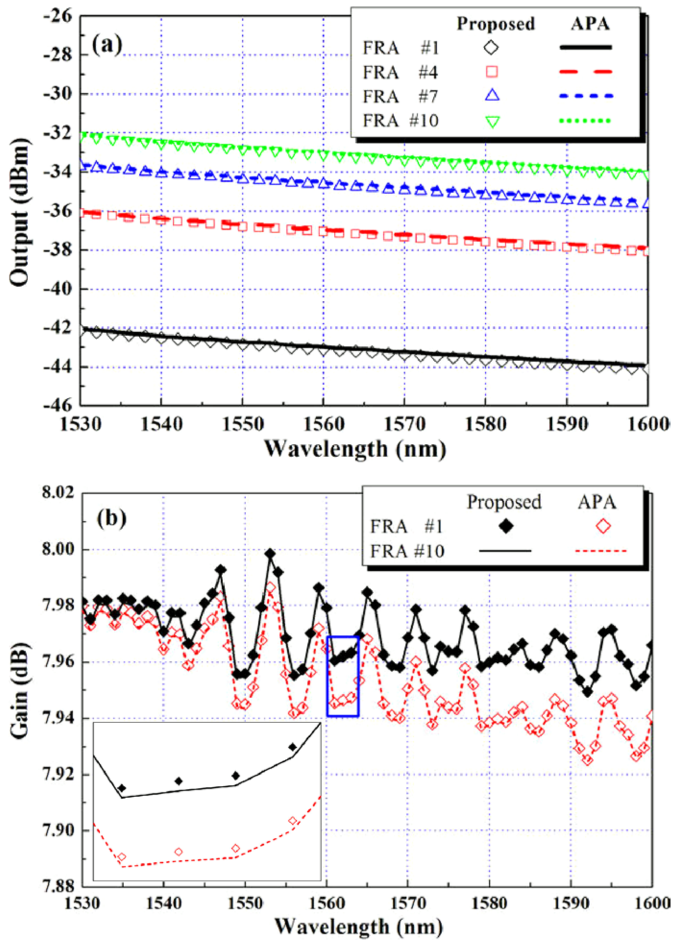

Fig. 5. (a) Accumulated noise power, (b) signal Raman on/off gain in transmission link with concatenated FRAs, resolution bandwidth = 0.5 nm.

(i) the amount of gain error between the signal gain and target spectrum—equivalent to the shooting method in one form or another—with tracking algorithms by pump grouping/simulated annealing [11,12], or (ii) rescaled pump power integrals obtained from the numerical integration of coupled differential equations/direct measurements [7,13–15]. Even if it should be possible to obtain the required set of pump powers/wavelengths following either of these different optimization procedures, all of these aforementioned approaches require time-consuming process of repetitive numerical integrations for coupled ODE [7,12,13] or repetitive measurement [11,14,15] including all of the involved waves.

With the constructed formulation of the Raman equation described in Section 2.2, we show here that highly accurate estimation of pump powers and fast construction of gain profiles can be achieved with much less effort, while still keeping all the Raman interaction effects in the calculation. For this, we first rewrite the expression for Raman on/off gain in Eq. (8), keeping the signal gain term only,

$$G_{i=(M+1)\dots N} = \sum_{j=1}^{M+N} g_{ji} \cdot L_{\mathrm{eff},j}(L) \cdot P_j(0), \qquad \vec{G}_{\mathrm{S}} = \tilde{T}_{\mathrm{P}} \times \vec{P}_{\mathrm{P}} + \tilde{T}_{\mathrm{S}} \times \vec{P}_{\mathrm{S}}, \tag{9}$$

where

$$\vec{G}_{\mathrm{S}} = \begin{bmatrix} G_{M+1} \\ G_{M+2} \\ \vdots \\ G_{M+N} \end{bmatrix},$$

$$\tilde{T}_{\mathrm{P}} = \begin{bmatrix} g_{1(M+1)}L_{\mathrm{eff},1}(L) & g_{2(M+1)}L_{\mathrm{eff},2}(L) & \cdots & g_{M(M+1)}L_{\mathrm{eff},M}(L) \\ g_{1(M+2)}L_{\mathrm{eff},1}(L) & g_{2(M+2)}L_{\mathrm{eff},2}(L) & \cdots & g_{M(M+2)}L_{\mathrm{eff},M}(L) \\ \vdots & \vdots & \vdots & \vdots \\ g_{1(M+N)}L_{\mathrm{eff},1}(L) & g_{2(M+N)}L_{\mathrm{eff},2}(L) & \cdots & g_{M(M+N)}L_{\mathrm{eff},M}(L) \end{bmatrix},$$

$$\vec{P}_{\mathrm{P}} = \begin{bmatrix} P_1(0) \\ P_2(0) \\ \vdots \\ P_M(0) \end{bmatrix},$$

$$\tilde{T}_{\mathrm{S}} = \begin{bmatrix} g_{(M+1)(M+1)}L_{\mathrm{eff},(M+1)}(L) & g_{(M+2)(M+1)}L_{\mathrm{eff},(M+2)}(L) & \cdots & g_{(M+N)(M+1)}L_{\mathrm{eff},(M+N)}(L) \\ g_{(M+1)(M+2)}L_{\mathrm{eff},(M+1)}(L) & g_{(M+2)(M+2)}L_{\mathrm{eff},(M+2)}(L) & \cdots & g_{(M+N)(M+2)}L_{\mathrm{eff},(M+N)}(L) \\ \vdots & \vdots & \vdots & \vdots \\ g_{(M+1)(M+N)}L_{\mathrm{eff},(M+1)}(L) & g_{(M+2)(M+N)}L_{\mathrm{eff},(M+2)}(L) & \cdots & g_{(M+N)(M+N)}L_{\mathrm{eff},(M+N)}(L) \end{bmatrix},$$

$$\vec{P}_{\mathrm{S}} = \begin{bmatrix} P_{M+1}(0) \\ P_{M+2}(0) \\ \vdots \\ P_{M+N}(0) \end{bmatrix}.$$

As mentioned before, here M is the number of pumps, and N is the number of signal waves.

From this, we start the gain design procedure for multi pumped RFA, by defining the target gain $\vec{G}_{\mathrm{T}}$ under a given set of constraints (bandwidth, flatness, available pump numbers, etc.). The following steps are used to practically acquire the solution set for a given problem stated above.

Step 1. Initial condition setup

First, considering the nature of adiabatic expansion where we treat $g_{ji} \times P_j(0) \times L_{\mathrm{eff},j}(\vec{z}_k)$ in Eq. (6) as a perturbation parameter, where $\tilde{L}^{(0)}_{\mathrm{eff},j}(\vec{z}_k)$ should be equal to

$(1 - \exp(\mp\alpha_j \vec{z}_k))/\alpha_j$. With $\tilde{L}^{(0)}_{\mathrm{eff},j}(\vec{z}_k)$, it is possible to get initial estimations for transfer matrices $\tilde{T}^{(0)}_{\mathrm{P}}$ and $\tilde{T}^{(0)}_{\mathrm{S}}$. By substituting the pre-determined target gain $\vec{G}_{\mathrm{T}}$ to Eq. (9), the initial guess of the required pump power $\vec{P}^{(0)}_{\mathrm{P}}$ can be obtained by $\vec{P}^{(0)}_{\mathrm{P}} = (\tilde{T}^{(0)}_{\mathrm{P}})^{-1}(\vec{G}_{\mathrm{T}} - \tilde{T}^{(0)}_{\mathrm{S}} \vec{P}_S)$, where signal power $\vec{P}_{\mathrm{S}}$ is the fixed boundary value inversely determined form the target gain $\vec{G}_{\mathrm{T}}$ and pre-determined input signal power.

Step 2. Calculation of higher-order terms

Substituting the $\vec{P}^{(0)}_j(0)$ (constructed by $\vec{P}^{(0)}_{\mathrm{P}}$ and $\vec{P}_{\mathrm{S}}$) and $\tilde{L}^{(0)}_{\mathrm{eff},j}(\vec{z}_k)$ into (6), effective lengths are updated to new values $\tilde{L}^{(1)}_{\mathrm{eff},j}(\vec{z}_k)$, which are then used to get updated matrices $\tilde{T}^{(1)}_{\mathrm{P}}$ and $\tilde{T}^{(1)}_{\mathrm{S}}$. From this, $\vec{P}^{(1)}_{\mathrm{P}}$ can be obtained by $\vec{P}^{(1)}_{\mathrm{P}} = (\tilde{T}^{(1)}_{\mathrm{P}})^{-1}(\vec{G}_{\mathrm{T}} - \tilde{T}^{(1)}_{\mathrm{S}} \vec{P}_{\mathrm{S}})$.

Step 3. Reiteration

Reiterating Step 2 for higher orders, the final solution set can be obtained.

Several design examples are shown in Figs. 6 and 8. For the example in Fig. 6, we set $\vec{G}_{\mathrm{T}}$ to 8 dB over the 70 nm (1530–1600 nm) spectral range. Considering practical restrictions in the pump WDM wavelength allocation, 16 equally spaced, counter-directional pump waves at 1420–1495 nm with 5 nm spacing were used. 71 waves at $-3\ \mathrm{dB\,m/ch}$ input power (1 nm spacing, 1530–1600 nm) were also assumed. 37 km of DSF with large Raman gain coefficients was used to test the validity of the algorithm.

Figure 6 shows the target gain (open symbol) $\vec{G}_{\mathrm{T}}$, and gain profiles generated by using the pump powers obtained at each stage of the iteration process (Steps 1–3). Figure 7 illustrates the typical trace of the pump evolution at each iteration step. As can be seen from the figure, after fifth iteration steps, the pump evolution sufficiently converges to that of a real value, and the gain curve excellently overlaps that of an ideal target gain. The convergence error from the iteration procedure becomes almost negligible after fifth iteration steps. The observed absolute error between target gain and the iteratively obtained gain profile after the fifth iteration steps was smaller than 0.08 dB over the whole 70 nm

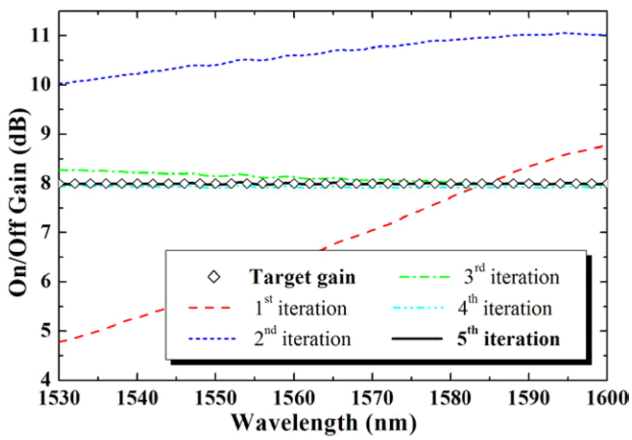

Fig. 6. On/off gain profiles of FRA obtained from the results at each iteration process.

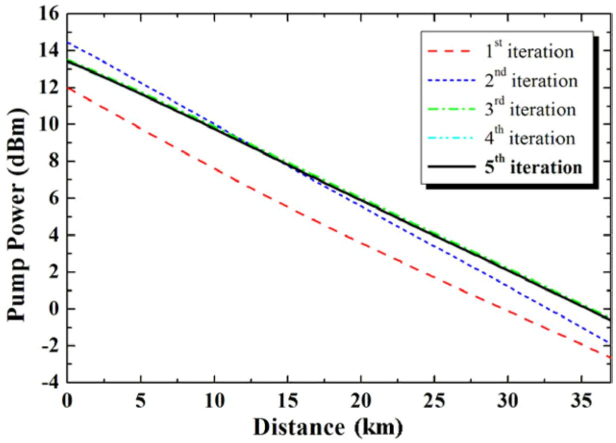

Fig. 7. Pump evolutions of FRA obtained from the results at each iteration process.

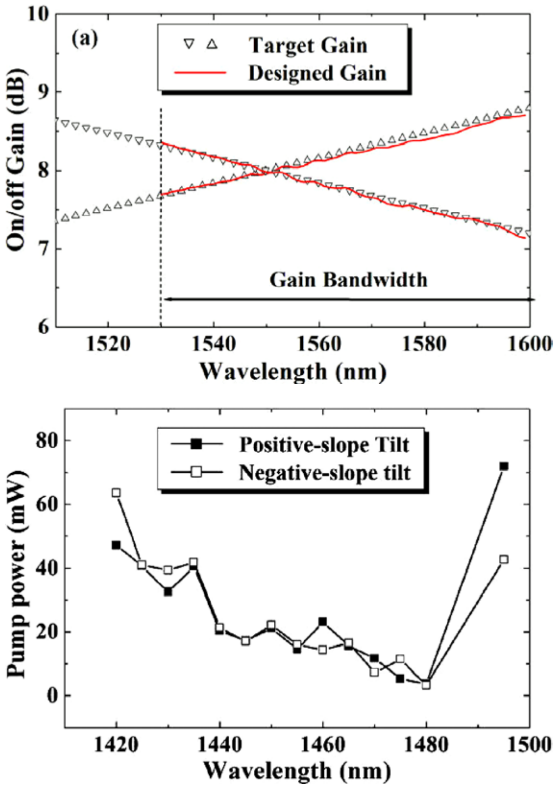

Fig. 8. Examples of gain design with (a) tilted (b) convex/concave target gain profile, and the corresponding pump power found by algorithm.

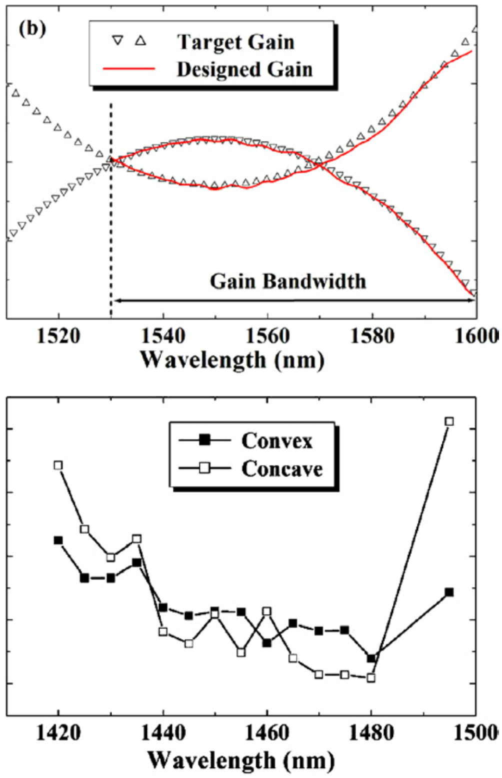

Fig. 8. (Continued.)

gain spectral range. Naturally, the level of gain accuracy could be further improved with additional iteration steps by monitoring the convergence of the average gain difference by each iteration step $\langle \Delta G \rangle_{AVG}$, but considering most of the practical applications under experimental error, five iteration step was generally sufficient. The required computation time to obtain this result after five steps of iteration was less than 1 s with a conventional PC (2.0 GHz CPU clock). For comparison, the common approach using direct integration of the Raman amplifier differential equation usually takes minutes for the whole procedure—without ASE and Rayleigh scattering effect [7], or even for a single scan—including ASE and Rayleigh scattering [13].

This unprecedented level of convergence speed is attributed to the following: (1) removal of the use of time-consuming coupled ODE equations in the optimization process, (2) transformation of coupled Raman equations into closed integral equation form, which enables the solution to be found along the iteration axis not the fiber propagation axis, (3) matrix formulation for both of the signal SRS effect and effective length iteration equation, enabling fast numerical process in the software, and (4) simultaneous application of signal SRS effect and pump integral update in every iteration step.

Figure 8 shows the design examples applied with this algorithm for various shapes of ideal target gain profiles (under identical setting as that of Fig. 6).

2.4. Application example 3: Gain clamping under channel reconfiguration

With technological advancement for the optical link equipped with dynamic lambda channel routing function, there have been many efforts to develop the control method for an optical amplifier to cope with input power variation induced by WDM channel add/drop. To assess the FRA-transient related issues such as cross gain modulation, signal stimulated Raman scattering (SSRS), and pump-to-pump interaction, numerical and experimental studies have been carried out [16–19]. Though previous the gain control method based on pump grouping [11], ASE/gain slope measurement [20], OTDR [14], linear matrix method [15], closed form expansion [8] in steady-state could provide some clues for the method to keep constant gain under channel add/drop condition, still a clear algorithm for the wideband FRA with large number of multi-pump/signal have not been proposed, especially in deep saturation regime where pump depletion/SSRS effects manifest.

Here, we apply the gain design algorithm described in Section 2.3 to the gain clamping problem as another application example to find out the required pump power set under the dynamic network reconfiguration environment. For this purpose in applying the technique described in Section 2.3, it is worth to note that to obtain a stable and reasonable solution, the algorithm should be processed with not only surviving signal channels but also with dropped signal channels, while naturally treating the power of dropped signal channel as zero.

As an example, a wide-band FRA providing 11.8 dB average on/off gain to the 80 C/L-band WDM signal channels has been constructed using the algorithm presented before (C-band: 40 channel, 1529.2–1560.4 nm, L-band: 40 channel, 1570.0–1601.2 nm with 100 GHz spacing, $-10\ \mathrm{dB\,m/channel}$). The required pump powers for the seven pumps (1420–1470 nm with 10 nm spacing and 1 additional pump at 1490 nm) were 135, 110, 55, 48, 51, 9, 84 mW, respectively.

Figure 9 shows the gain spectrum of FRA under channel drop in a different manner with/without the pump adjustment. As illustrated, successful gain clamping has been achieved with the proper adjustment of pump powers, which were found applying the algorithms described in Section 2.3. To compare, 0.5 dB of excursion in the gain have been observed for surviving channels (40 channel drop out of 80 channel), when no pump control has been applied. The required computation time to obtain this result was almost similar to the one in Section 2.3.

2.5. Application example 4: Analytic solution for gain clamping

Even if the gain-clamping problem can be easily addressed with the methods described in Sections 2.3 and 2.4, the dynamic control of FRA requires an algorithm that is much faster than the order of seconds. Restricting the given problem to practical applications, where we use a small signal for the input of RFA, we now show that the simplified analytic solution enabling faster calculation of required pump power set could be obtained. To begin, we rewrite the FRA gain in Eq. (8) to the following matrix form that the pump and signal gain parts are separated, by using the similar formalism in Eq. (9),

$$\begin{bmatrix} G_\mathrm{p} \\ G_\mathrm{s} \end{bmatrix} = \begin{bmatrix} C_\mathrm{pp} & C_\mathrm{sp} \\ C_\mathrm{ps} & C_\mathrm{ss} \end{bmatrix} \begin{bmatrix} I_\mathrm{p} \\ I_\mathrm{s} \end{bmatrix}, \tag{10}$$

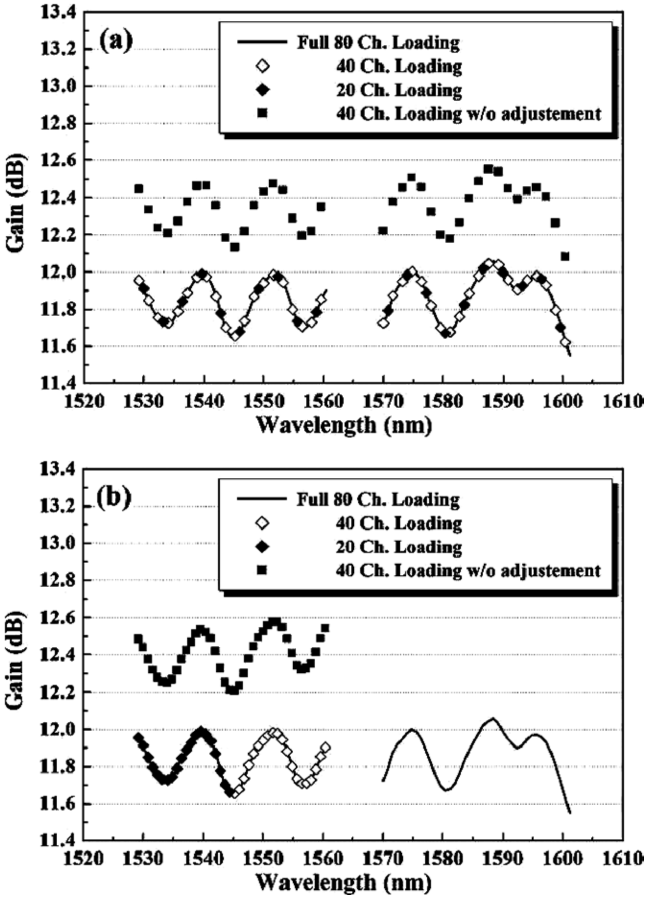

Fig. 9. Gain spectrum with/without the adjustment of pump power: (a) interleaved channels dropped out, (b) red-shifted channels dropped.

where G_p is a $M \times 1$ vector representing the Raman gain for pumps, and I_p and I_s are the vector constructed from the power integral (equal to $P(0) \times L_{eff}(L)$) of pumps and signals, respectively. Comparing to Eq. (8), it is easy to see that C is a constant matrix composed of elements g_{ji} (equivalently, same as matrix T without L_{eff}). Under this formulation, the physical meanings of the sub-matrix C_{ij} become clear: C_{pp} = pump-to-pump interaction, C_{ss} = signal-to-signal interaction (signal SRS), C_{sp} = signal-to-pump interaction (pump depletion), and C_{ps} = pump-to-signal interaction (signal amplification).

On the other hand, we note that the following equation should be satisfied, if one wants to keep the gain of the surviving channel unchanged under the channel reconfiguration environment,

$$\Delta G_s = C_{ps}\Delta I_p + C_{ss}\Delta I_s = 0, \tag{11}$$

$$\Delta I_p = -(C_{ps})^{-1} C_{ss}\Delta I_s, \tag{12}$$

where ΔG_s, ΔI_s, and ΔI_p are the change in the signal gain, change in the integral of the signal and pump power, respectively. Applying Eq. (12) to the pump gain in Eq. (10), the relation between ΔG_p and ΔI_s becomes

$$\Delta G_p = C_{pp}\Delta I_p + C_{sp}\Delta I_s = \left\{-C_{pp}(C_{ps})^{-1}C_{ss} + C_{sp}\right\}\Delta I_s. \tag{13}$$

Now, restricting the given problem to the undepleted pump regime, the signal power evolutions along the fiber should not be different from that of original operating condition even after the channel reconfiguration. In this approximation, ΔI_s can be easily determined, since ΔI_s of dropped channels are naturally $-I_s$, and ΔI_s of surviving channels are zero (tested error $\Delta I_s/I_s$ was less than 0.2 dB for 78 channels dropping out of 80, for examples in the previous/following settings).

Meanwhile, from the definition of effective length, the variation of pump effective length $\Delta L_{\mathrm{eff,p}}$ can be calculated by using the variation of pump gain ΔG_p as follows:

$$L_{\mathrm{eff,p}} + \Delta L_{\mathrm{eff,p}} = \int_0^L \left[\frac{(P_p(0) + \Delta P_p(0))\exp\{-\alpha_p z + (G_p(z) + \Delta G_p(z))\}}{P_p(0) + \Delta P_p(0)}\right] dz,$$

$$\Delta L_{\mathrm{eff,p}} = -L_{\mathrm{eff,p}} + \int_0^L \exp\left\{-\alpha_p z + \left(G_p(z) + \Delta G_p(z)\right)\right\} dz. \tag{14}$$

Again, employing the definition of effective length, the variation of pump power integral and pump gain can be related to the variation of the pump power $\Delta P_p(0)$ (note, this is the final target solution)—as follows:

$$L_{\mathrm{eff,p}} + \Delta L_{\mathrm{eff,p}} = \frac{\int_0^L P_p(z) + \Delta P_p(z)\,dz}{P_p(0) + \Delta P_p(0)} = \frac{I_p + \Delta I_p}{P_p(0) + \Delta P_p(0)},$$

$$\Delta P_p(0) = \frac{\Delta I_p - \Delta L_{\mathrm{eff,p}} P_p(0)}{L_{\mathrm{eff,p}} + \Delta L_{\mathrm{eff,p}}}, \quad I_p = L_{\mathrm{eff,p}} P_p(0), \tag{15}$$

where ΔI_p is a known quantity from Eq. (12), $P_p(0)$ is the input pump power before the reconfiguration, and $L_{\mathrm{eff,p}}$ is the effective length from the initial setup (which we already know).

Because this analytic approach does not require any iteration process—in contrast to the examples of Section 2.4—but only simple calculation from the known parameters of FRA (before the reconfiguration) and changes in the signal power, the whole procedure for the search of the proper pump power sets required for the gain control can be achieved with orders of higher speed ($\sim$20 μs) when compared to the method based on iteration approach described in Sections 2.3 and 2.4 ($\sim$1 s).

As an example, for the identical reconfiguration scenario used in Section 2.4, we calculated the pump power sets from the above equations. The gain spectrums from this adjusted pump power set is illustrated in Fig. 10. Up to the input power change of 6 dB (60 from 80 channel drop-out), the residual gain excursion was suppressed within 0.2 dB with this gain clamping method. It is worth to note that, even if the small signal approximation has been applied to get the above analytic result, the observed gain error was still smaller than 0.5 dB when the same test was carried out with an increased signal power of -5 dB m/ch.

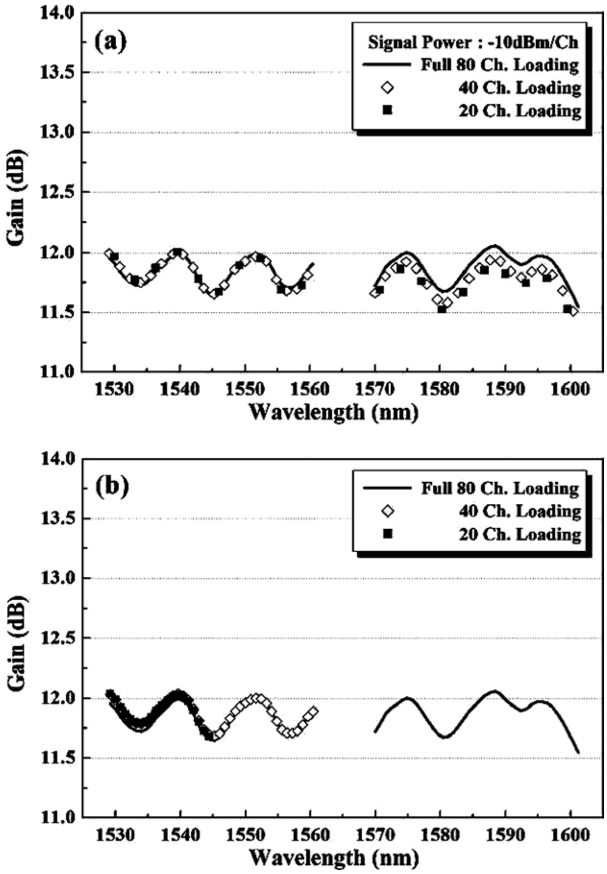

Fig. 10. Gain spectrum with pump adjustment by analytic derivation: (a) interleaved channels dropped out, (b) red-shifted channels dropped.

3. Conclusion

We introduced a novel FRA modeling framework by transforming the complicated differential Raman equation into a closed integral/matrix form. By taking the effective length as the interim target solution and updating its value along the iteration axis, Raman gain and pump/signal power evolution can be obtained with orders of magnitude increase in convergence speed and excellent accuracy when compared to the previous, coupled ODE based approaches. Application of this formalism to the problem of (i) gain prediction with a given parameters, (ii) gain spectrum engineering for the search of optimum pump power set under the given constraints, (iii) gain clamping problem for the channel reconfiguration, and (iv) derivation of analytic formula for the faster FRA dynamic control have been addressed, with excellent accuracy and conversion speed to assist the high-level, practical design of the FRA.

References

[1] M.N. Islam, Raman amplifier for telecommunications, J. Lightwave Technol. 8 (2002) 548–559.
[2] Y. Emori, S. Kado, S. Namiki, Broadband flat-gain and low-noise Raman amplifier pumped by wavelength-multiplexed high-power laser diodes, Opt. Fiber Technol. 8 (2002) 107–122.
[3] K. Rottwitt, M. Nissov, F. Kerfoot, Detailed analysis of Raman amplifiers for long haul transmission, in: Proceedings of Optical Fiber Communication Conference, 1998, pp. 30–31, paper TuG1.
[4] H. Kidorf, K. Rottwitt, M. Nissov, M. Ma, E. Rabarijaona, Pump interactions in a 100-nm bandwidth Raman amplifier, IEEE Photon. Technol. Lett. 11 (1999) 530–532.
[5] B. Min, W.J. Lee, N. Park, Efficient formulation of Raman amplifier propagation equations with average power analysis, IEEE Photon. Technol. Lett. 12 (2000) 1486–1488.
[6] I. Mandelbaum, M. Bolshtyansky, Raman amplifier model in single-mode optical fiber, IEEE Photon. Technol. Lett. 15 (2003) 1704–1706.
[7] V.E. Perlin, H.G. Winful, Optimal design of flat-gain wide-band fiber Raman amplifiers, J. Lightwave Technol. 20 (2002) 250–252.
[8] J. Park, P. Kim, J. Park, H. Lee, N. Park, Closed integral form expansion of Raman equation for efficient gain optimization process, IEEE Photon. Technol. Lett. 16 (7) (2004) 1649–1651.
[9] L.K. Choi, J. Park, P. Kim, J. Park, N. Park, Closed integral form expansion of Raman equation and its iteration method for highly efficient Raman amplifier analysis, in: Proceedings of Optoelectronics and Communications Conference, Yokohama, 2004, paper 13P-85.
[10] K. Rottwitt, A.J. Stentz, Raman amplification in lightwave communication systems, in: I.P. Kaminow, L. Tingye (Eds.), Optical Fiber Telecommunications IVA, vol. 217, Academic Press, San Diego, 2002.
[11] Y. Emori, S. Kado, S. Namiki, Simple gain control method for broadband Raman amplifiers gain-flattened by multi-wavelength pumping, in: Proceedings of European Conference on Optical Communication, vol. 2, 2001, pp. 158–159, paper TuA2.2.
[12] M. Yan, J. Chen, W. Jiang, J. Li, J. Chen, X. Li, Automatic design scheme for optical-fiber Raman amplifiers backward-pumped with multiple laser diode pumps, IEEE Photon. Technol. Lett. 13 (2001) 948–950.
[13] A.R. Grant, Calculating the Raman pump distribution to achieve minimum gain ripple, J. Quant. Electron. 38 (2002).
[14] P. Kim, J. Park, H. Yoon, J. Park, N. Park, In-situ design method for multi-channel gain of distributed Raman amplifier with the multi-wave OTDR, IEEE Photon. Technol. Lett. 14 (2002) 1683–1685.
[15] W. Zhang, X. Feng, J. Peng, X. Liu, A simple algorithm for gain spectrum adjustment of backward-pumped distributed fiber Raman amplifiers, IEEE Photon. Technol. Lett. 16 (2004) 69–71.
[16] S. Gray, Transient gain dynamics in wide bandwidth discrete Raman amplifiers, in: Proceedings of Optical Fiber Communication Conference, 2002, pp. 512–513, paper ThR2.
[17] A. Bononi, M. Papararo, M. Fuochi, Transient gain dynamics in saturated Raman amplifiers, Opt. Fiber Technol. 10 (2004) 91–123.
[18] M. Karasek, J. Kanka, P. Honzatko, P. Peterka, Modelling of a pump-power-controlled gain-locking system for multi-pump wideband Raman fibre amplifiers, in: Optoelectronics, IEEE Proceedings, vol. 151, 2004, pp. 74–80.
[19] A. Bononi, M. Fuochi, Transient gain dynamics in saturated Raman amplifiers with multiple counter-propagating pumps, in: Proceedings of Optical Fiber Communication Conference, 2003, pp. 439–441, paper ThC3.
[20] M. Sobe, Y. Yano, Automatic pump power adjustment for gain-flattened multi-wavelength pumped Raman amplifier, in: Proceedings of Optical Fiber Communication Conference, 2002, pp. 63–65, paper TuJ5.